RSC Advances

PAPER

View Article Online
View Journal | View Issue



Cite this: *RSC Adv.*, 2020, **10**, 21009

# Uniform Cu/chitosan beads as a green and reusable catalyst for facile synthesis of imines *via* oxidative coupling reaction†

Threeraphat Chutimasakul, Pakamon Na Nakhonpanom, Warinda Tirdtrakool, Apichai Intanin, Thanthapatra Bunchuay, Rattikan Chantiwas and Jonggol Tantirungrotechai *

Received 30th April 2020
Accepted 25th May 2020

DOI: 10.1039/d0ra03884a

rsc.li/rsc-advances

A nonprecious metal and biopolymer-based catalyst, Cu/chitosan beads, has been successfully prepared by using a software-controlled flow system. Uniform, spherical Cu/chitosan beads can be obtained with diameters in millimeter-scale and narrow size distribution (0.78 ± 0.04 mm). The size and morphology of the Cu/chitosan beads are reproducible due to high precision of the flow rate. In addition, the application of the Cu/chitosan beads as a green and reusable catalyst has been demonstrated using a convenient and efficient protocol for the direct synthesis of imines *via* the oxidative self- and cross-coupling of amines (24 examples) with moderate to excellent yields. Importantly, the beads are stable and could be reused more than ten times without loss of the catalytic performance. Furthermore, because of the bead morphology, the Cu/chitosan catalyst has greatly simplified recycling and workup procedures.



## Introduction

The development of green and effective heterogeneous catalysts has long been a focus for many researchers due to their sustainable advantages in terms of recyclability and waste reduction. One of the key efforts in the study is to stabilize metal active centers using supporting materials such as inorganic oxides or organic polymers. Particularly, biopolymers have emerged as promising catalytic supports because they are cheap, biodegradable, and non-toxic. Chitosan is the *N*-deacetylated derivative of chitin found in crustacean shells and exoskeletons of insects. The structure of chitosan contains hydroxyl and amino functional groups, rendering it useful for metal coordination as a supramolecular ligand.[1] In addition, the solubility of chitosan provides flexibility for casting into powders, fibers, films, and beads.[2–4]

Transition metal functionalized chitosan has recently received tremendous attention for heterogeneous catalysis applications.[5] Even though the use of heterogeneous catalysts in the liquid phase can aid considerably in the separation and reuse of the catalysts, the recovery process by filtration or centrifugation can be labor-intensive, and the loss of catalysts mass during the separation is inevitable for nanoscale particles. Therefore, heterogeneous catalysts in the forms of pellets or beads are preferred, especially for industry. Millimeter-sized chitosan beads can be readily prepared by manually dropping an acidic chitosan solution into a basic solution. However, this procedure limits practical application because of the difficulty in scaling-up, low production rate, as well as the challenge to control narrow size distribution and uniform shape. A flow system with computer control should be able to circumvent these problems.

Chitosan incorporated copper species have been reported as excellent catalysts for reactions such as N-arylation of amines,[6] borylation of α,β-unsaturated acceptors,[7] C–S and C–N coupling reactions,[8–10] and azide–alkyne cycloaddition.[11–13] In these reports, chitosan was functionalized to create coordination sites for copper centers, and the resulting chitosan supported copper catalysts were in the form of powders. Therefore, it is of interest to prepare Cu/chitosan beads by employing high precision flow rate generated by a flow system. Recently, we have reported a study on the development of a simple reversible-flow method comprising of a reversible-flow syringe pump with a 3-port switching valve and a holding coil for the preparation of micron-size Cu/chitosan beads.[14] The uniform distribution of size and shape of the catalyst beads with good production rate could be achieved. Thus, this preparation method and the obtained Cu/chitosan beads deserve further investigation.

Imines are not only crucial intermediates for the synthesis of organic compounds exhibiting biological activities, but also can be used as dyes, fragrances, catalysts, and polymer stabilizers.[15,16] Conventionally, an imine can be synthesized from the

*Department of Chemistry, Center of Excellence for Innovation in Chemistry, Faculty of Science, Mahidol University, Bangkok 10400, Thailand. E-mail: jonggol.jar@mahidol.ac.th; jonggol@gmail.com*

† Electronic supplementary information (ESI) available. See DOI: 10.1039/d0ra03884a

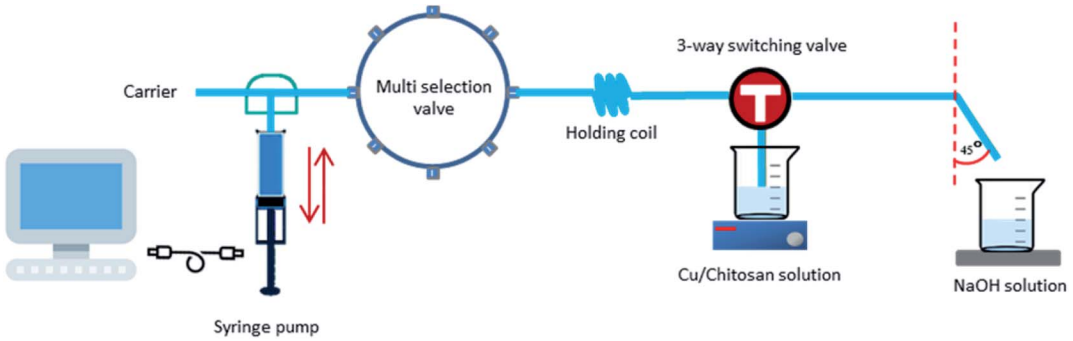


Fig. 1 The flow system with software controller using a reversible-flow syringe pump with a 3-port switching valve and a holding coil for preparation of Cu/chitosan beads.

condensation of a primary amine and a carbonyl compound in the presence of an acid catalyst. This acid-catalyzed method provides good yields, but often requires harsh reaction conditions and prolonged reaction times. Moreover, carbonyl compounds, especially aldehydes, are reactive and not easy to handle or store. The oxidative coupling of primary amines is one of the promising alternatives to synthesize various imine products.[17] Homogeneous and heterogeneous catalysts based on V,[18] Mn,[19,20] Co,[21,22] Ru,[23] Pd,[24] Ir,[25] Au,[26–28] and Ce[29] have been proposed to catalyze this reaction. Over the past decades, researchers are very much interested in the copper-based catalysts for the oxidative coupling of primary amines.[30–44] However, many problems have not been resolved effectively. For example, the reactions require the use of additives, harsh reaction conditions, long reaction time, and complicated catalyst preparation. Therefore, it is of immense interest to develop a new heterogeneous copper-based catalyst that is efficient, convenient, cheap, eco-friendly, and reusable for the oxidative coupling of amines to form a variety of imine compounds.

For these reasons, our research effort has been focused on the development of Cu/chitosan as a simple, eco-friendly, and inexpensive heterogeneous catalyst. Herein, we report an automated system to prepare stable Cu/chitosan beads, and the preparation conditions were examined. These Cu/chitosan beads were well characterized and employed as an efficient and recyclable heterogeneous catalyst for the oxidative coupling of various amines. The beads could be easily separated from the reaction medium by simple decantation, and the catalyst can be reused at least ten times with no significant loss of activity. This convenient approach for the preparation of catalyst beads could be beneficial to both synthetic chemistry and chemical industrial processes.

## Experimental

$Cu(OAc)_2$ (98%), $CuCl_2$ (98%), CuO (98%), and CuI (98%), chitosan (190–310 kDa, 75–85% deacetylated), *tert*-butyl hydroperoxide (TBHP, 5.0–6.0 M in decane), hexamethylbenzene (99%), and all amine derivatives were purchased from Sigma-Aldrich and used as received. NaOH (99%), HCl (37%), and all organic solvents were of analytical grade and obtained from RCI Labscan. De-ionized (DI) water from Nanopure® Analytical Deionization Water System with an electronic resistance ≥ 18.2 MΩ cm was used in all experiments.

### Preparation of Cu/chitosan beads

Chitosan (170 mg) was dissolved in 0.15 M HCl (10 mL), and the solution was stirred at room temperature for 30 min. A 2 mL aqueous copper solution (0.25, 0.50, or 0.75 M of $Cu(OAc)_2$, $CuCl_2$, CuO, or CuI) was gradually added to the acidic chitosan solution, and the obtained viscous solution of Cu/chitosan was stirred for 45 min to allow complexation between copper species and chitosan. The freshly prepared Cu/chitosan solution was first drawn into the holding coil by the syringe pump operating in the reverse-flow direction. The Cu/chitosan solution was then slowly pushed by the syringe pump into an aqueous NaOH bath leading to the formation of Cu/chitosan hydrogel droplets (Fig. 1). The computer-controlled sequential operational steps of the reversible-flow system are summarized in Table S1.† Finally, the resulting hydrogel beads were washed five times with DI water, filtered, and dried at room temperature to obtain black Cu/chitosan beads.

### Characterization

The crystal structure was determined by powder X-ray diffraction (XRD) using a Bruker D8 Advance diffractometer with Cu Kα ($\lambda = 1.5406$ Å) X-rays for $2\theta = 20.0$–$80.0°$. The morphology of Cu/chitosan beads was examined by scanning electron microscopy (SEM, Hitachi S-2500) operated at 15 kV. Energy-dispersive X-ray (EDX) analysis was employed to obtain elemental mapping using silicon drift detector coupled with SEM system. X-ray photoelectron spectroscopy (XPS) was carried out on Axis Ultra DLD spectrometer at 15 kV, 10 mA, and 150 W. The spectra were calibrated by referencing the C 1s line at BE = 285 eV. Electron spin resonance (ESR) spectra were taken in the X-band using a Bruker ELEXYS 500 instrument. The ESR signals were registered at a microwave power of 20 mW and modulation amplitude of 4.0 G in the field range of 2500–4000 G with a sweep time of 40 s. Thermogravimetric analyses (TGA, SDT 2960) were carried out in a temperature range of 30–800 °C with a heating rate of 20 °C $min^{-1}$ under air flow. The elemental composition of samples was determined by inductively coupled plasma-mass spectrometry (ICP-MS, Perkin-Elmer SCIEX-ELAN

 

600) with emission line at 324.75 nm. The samples were digested by nitric acid to a clear solution before the measurement. The elemental calibration curves were prepared in the range of 1–100 ppm.

### Oxidative coupling of amines

In a typical reaction, Cu/chitosan beads, amine derivatives, TBHP, hexamethylbenzene as an internal standard, and solvent were added to a reaction tube. For the cross-coupling reaction, another amine derivative was added to the reaction. The mixture was heated at an appropriate temperature for a desired reaction time. Then, the reaction mixture was quickly cooled to room temperature, and the catalyst beads were removed. The liquid mixture was extracted with ethyl acetate ($3 \times 2$ mL), and the volume was adjusted to 10 mL. The obtained solution was analyzed by gas chromatography-mass spectrometry (GC-MS, Agilent Technologies 7890A instrument with 5975C inert XL MSD) and/or $^1$H nuclear magnetic resonance spectroscopy ($^1$H NMR in $CDCl_3$, Bruker DPX-400) to obtain conversion and yield. In the recycle experiment, Cu/chitosan beads were reused after washing with ethyl acetate without drying.

## Results and discussion

### Preparation of Cu/chitosan beads

Even though at the macroscopic level, all resulting Cu/chitosan beads appear black and spherical after drying (Fig. 2), the microscopic morphology of the beads depends on the types of copper precursor used in the preparation as illustrated by SEM images in Fig. 3. This is because the viscosity of the Cu/chitosan solution plays a crucial role in the formation of the spherical beads. Under the condition studied, the beads derived from $Cu(OAc)_2$ have the most spherical shape compared to the others. In addition, the preparation of Cu/chitosan beads by our flow system described in Fig. 1 led to greater uniformity of particle shape with narrower size distribution than the manual dropping method ($0.78 \pm 0.04$ mm *vs.* $0.92 \pm 0.09$ mm) due to greater precision of flow rate control in the production of Cu/chitosan hydrogel droplet. SEM-EDX analysis also confirmed the uniform elemental distribution throughout the bead surface (Fig. 4).

In addition to the type of copper precursor, other parameters such as the concentrations of chitosan solution and NaOH bath as well as the flow rate can affect the formation of the beads. An effective concentration of chitosan impacts gel formation. Low concentration of the acidic chitosan solution (*i.e.*, 0.50% w/v) failed to form hydrogel droplets due to its low viscosity. On the other hand, high viscosity of the chitosan solution (*i.e.*, 2.0% w/v) restricted flow-through of the chitosan solution into small i.d. tubing of the flow system. The concentration of NaOH receiving bath affected the rate of gelation and solidification which, in turn, influenced the size distribution of the beads; and 1 M NaOH solution provided the narrowest size distribution. However, the size distribution of the beads was not significantly different from the increasing flow rate, while the mean size of the beads increased with the flow rate. We could control the amount of Cu in the beads by varying the concentration of Cu solution (0.25–0.75 M). This parameter did not affect the mean particle size. Nevertheless, Cu content influenced the mechanical strength of the beads. At higher concentration (>0.5 M) of Cu solution, the obtained beads became more brittle and could be crushed by a magnetic bar during stirring in a liquid medium. From these results, we propose that the most suitable condition to produce Cu/

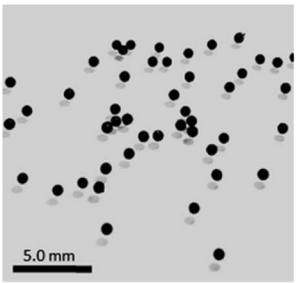


Fig. 2 Picture of spherical Cu/chitosan beads prepared from $Cu(OAc)_2$ with a mean particle size of $0.78 \pm 0.04$ mm.

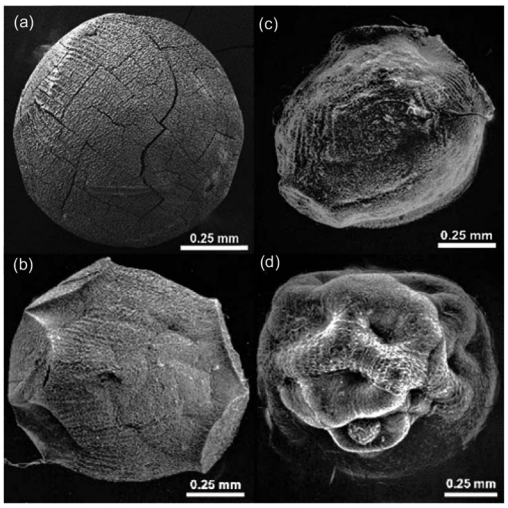


Fig. 3 SEM images of Cu/chitosan beads prepared from (a) $Cu(OAc)_2$, (b) CuO, (c) $CuCl_2$, and (d) CuI.

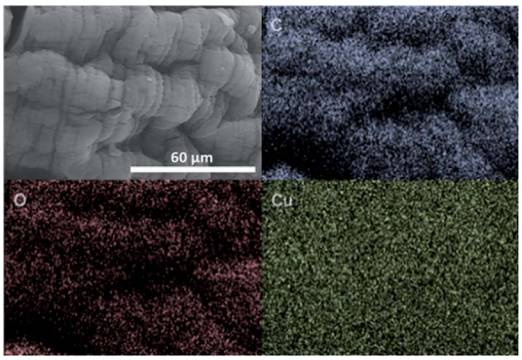


Fig. 4 Elemental mapping of Cu/chitosan beads prepared from $Cu(OAc)_2$.

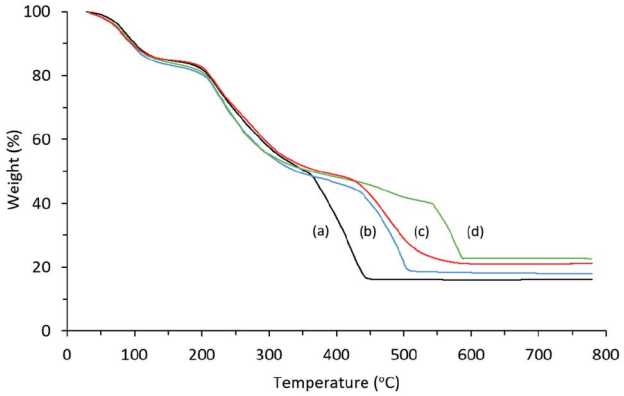


Fig. 5 TGA diagrams of Cu/chitosan beads prepared from (a) $Cu(OAc)_2$, (b) CuO, (c) CuI, and (d) $CuCl_2$.

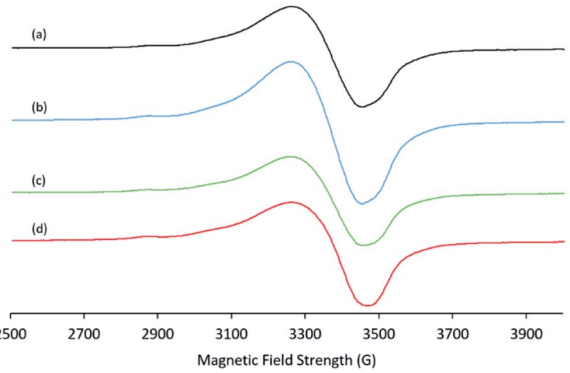


Fig. 7 ESR spectra of Cu/chitosan beads prepared from (a) $Cu(OAc)_2$, (b) CuO, (c) $CuCl_2$ and (d) CuI.

chitosan beads is to use 1.7% w/v acidic chitosan solution mixed with 0.25 M $Cu(OAc)_2$ solution as Cu/chitosan reservoir solution and to drop the Cu/chitosan solution into a 1.0 M NaOH receiving bath at a constant flow rate.

### Characterization of Cu/chitosan beads

The thermal property of Cu/chitosan beads was examined by TGA as shown in Fig. 5. The thermal decomposition behavior was similar to that of chitosan with CuO as final residues in all cases. The copper contents calculated from the residue weight loss were 12, 12, 14, 14% wt for the beads prepared from $Cu(OAc)_2$, CuO, $CuCl_2$, and CuI, respectively. These numbers are in good agreement with the values obtained from ICP-MS technique (11, 11, 13, and 12% wt, respectively).

The surface property of the beads was studied by XPS. The results revealed that the copper content on the beads prepared from $Cu(OAc)_2$ was 10% wt. This value is close to that found by ICP-MS technique (11% wt), implying good distribution of copper in the bulk and on the surface of the beads. High resolution XPS spectra in the region of C 1s, N 1s, O 1s, and Cu 2p are displayed in Fig. 6. The C 1s spectrum could be fitted with the binding energies of 284.7 (aliphatic carbon C–C, C–H, and C=C), 286.8 (–C–OH, –C–N, and C–O–C), and 289.6 eV (–COOH, N–C=O, and O–C–O) due to the chitosan structure.[45–48] Moreover, the N 1s spectrum consisted of the peak at 398.5 eV corresponded to amino group on chitosan (C–N) and the peak at 401.7 eV belong to $–N–H^+$ and $–NH_3^+$–Cu moieties.[45] The O 1s spectrum was deconvoluted into four peaks. The binding energies at 529.7, 531.2, 532.7, and 533.7 eV were assigned to (O–Cu), (O=C), (O–C and O–H), and (O–C–O), respectively.[47] These results suggested that the nitrogen and oxygen atoms of chitosan could chelate to copper species in the beads. The Cu 2p spectrum revealed two peaks at binding energies of 932.8 (Cu $2p_{3/2}$) and 938.9 eV (the Auger spectrum of the CuLMM transition), corresponding to copper(II) species.[47]

ESR spectroscopic results further confirm the presence of copper(II) species. The ESR spectra of Cu/chitosan beads exhibit a pattern with $g_{\|} = 2.268–2.273$ and $g_{\perp} = 2.090–2.093$ (Fig. 7). These $g$-values are comparable to those reported for the chitosan complexes formed with $Cu(NO_3)_2$ ($g_{\|}$ and $g_{\perp}$ values of 2.264 and 2.091, respectively).[49]

XRD patterns reveal the presence of crystalline CuO (JCPDS card no. 45-0937) as illustrated in Fig. 8. Even the sample prepared from CuI exhibited the XRD peaks of CuO. It is possible that Cu(I) species were oxidized to Cu(II) by ambient air under the condition employed in the preparation of the beads.

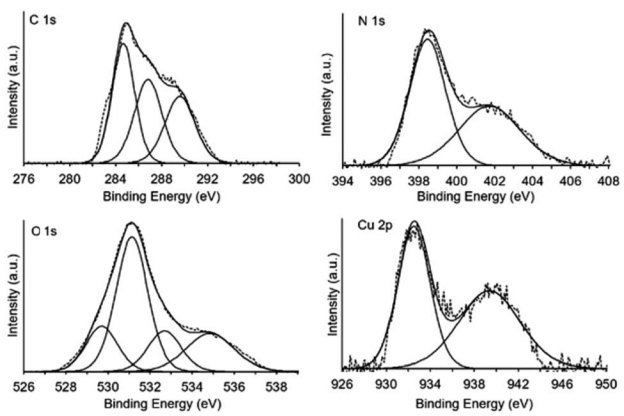


Fig. 6 XPS spectra of Cu/chitosan beads prepared from $Cu(OAc)_2$.

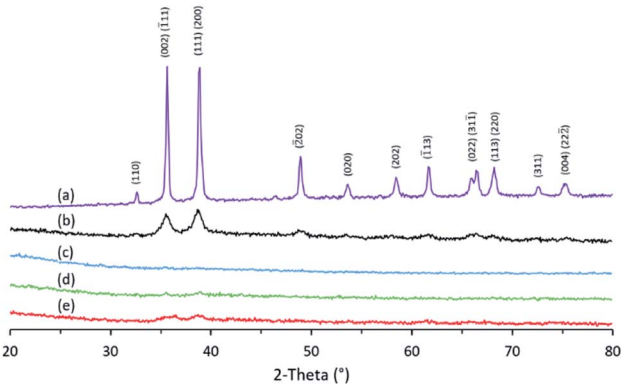


Fig. 8 XRD patterns of (a) copper(II) oxide (CuO, JCPDS card no. 45-093) and Cu/chitosan beads prepared from (b) $Cu(OAc)_2$, (c) CuO, (d) $CuCl_2$, and (e) CuI.

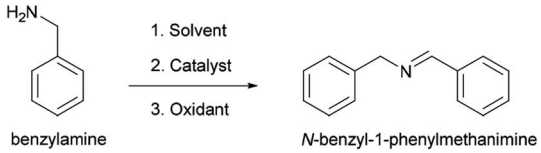


Scheme 1 The oxidative self-coupling reaction of benzylamine.

The sample prepared from $Cu(OAc)_2$ afforded the highest crystallinity compared to the others. The better crystallinity or faster crystallization rate of CuO in this sample may be responsible for the more spherical appearance of the beads (Fig. 3). To probe the functional groups of Cu/chitosan beads, all samples were subjected to FTIR spectroscopic studies. FTIR spectra of all beads display similar signal patterns to that of pure chitosan as shown in Fig. S2.†

### Oxidative coupling of amines by Cu/chitosan beads

Cu/chitosan beads were applied as a catalyst in the oxidative coupling of primary amines to their corresponding imines. Benzylamine was selected as a model starting substrate to investigate the effects of the copper precursor and the reaction parameters including solvent, temperature, and oxidizing agent on the catalytic performance (Scheme 1).

The oxidative coupling of benzylamine was performed in acetonitrile at 80 °C for 30 min with TBHP as the oxidizing agent. In the absence of Cu/chitosan catalyst, only 18% of benzylamine could be converted to imine (Table 1, entry 1). Likewise, if only chitosan beads were present, 18% conversion could be obtained (entry 2). However, in the presence of Cu/chitosan beads, up to 98% yield of imine could be achieved under the same reaction condition (entries 3–8). Therefore, the oxidative coupling of benzylamine requires Cu species to catalyze the reaction. The Cu content in the beads could be controlled from the initial concentration of Cu solution used in the preparation of Cu/chitosan beads. When the Cu content was higher, higher imine yield could be obtained (entries 3–5). Interestingly, the copper

Fig. 9 The catalytic reaction mixture of Cu/chitosan powder (left) and Cu/chitosan beads (right).

precursor strongly influences the product yield. With similar Cu loading, the beads prepared from $Cu(OAc)_2$ provided the highest yield of 98%, followed by the ones from $CuCl_2$ (87%), CuO (81%), and CuI (69%), respectively. It is possible that the residue acetate anion acts as a Lewis base and enhances the product yield in addition to supporting the spherical bead structure (Fig. 2). To further confirm the effect of the acetate anion on the catalytic performance, sodium acetate was added to the reaction mixture with Cu/chitosan beads prepared from $CuCl_2$; and the result shows that the imine yield could be raised from 86 to 94% (entries 8 and 9).

For comparison, $Cu(OAc)_2$ as well as the *in situ* mixture of $Cu(OAc)_2$ and chitosan beads were used as homogeneous analogs. Here, under the same reaction condition and time, full conversion of benzylamine was observed with 17–20% yield of the imine product (Table 1, entries 10 and 11). The low yield in these cases was caused by the formation of a by-product, benzaldehyde, from the hydrolysis of the imine after prolonged heating of the reaction mixture. Thus, the homogeneous $Cu(OAc)_2$ catalyst provided higher reaction rate for the oxidative coupling of benzylamine. However, the homogeneous catalyst is difficult to be separated from the reaction mixture and may cause contamination to the environment. When Cu/chitosan beads were crushed to powders and then used as a heterogeneous catalyst (entry 12), the reaction rate was also higher than

Table 1 Oxidative self-coupling reaction of benzylamine by various catalysts[a]

| Entry | Catalyst[b] | Cu loading[c] (mol%) | Conv.[d] (%) | Yield[d] (%) | TOF ($h^{-1}$) |
|---|---|---|---|---|---|
| 1 | No catalyst | — | 18 | 15 | — |
| 2 | Chitosan beads | — | 18 | 17 | — |
| 3 | Cu/chitosan beads ($Cu(OAc)_2$) | 1.8 | 65 | 57 | 73.7 |
| 4 | Cu/chitosan beads ($Cu(OAc)_2$) | 3.5 | >99 | 98 (91)[e] | 57.7 |
| 5 | Cu/chitosan beads ($Cu(OAc)_2$) | 4.5 | >99 | 96 | 44.4 |
| 6 | Cu/chitosan beads (CuO) | 3.4 | 81 | 80 | 55.3 |
| 7 | Cu/chitosan beads (CuI) | 3.7 | 69 | 63 | 36.8 |
| 8 | Cu/chitosan beads ($CuCl_2$) | 4.2 | 87 | 86 | 41.9 |
| 9 | Cu/chitosan beads ($CuCl_2$) + $CH_3COONa$ (0.5 mmol) | 4.2 | 96 | 94 | 46.2 |
| 10 | $Cu(OAc)_2$ + chitosan beads | 3.3 | >99 | 20 | 60.5 |
| 11 | $Cu(OAc)_2$ | 3.3 | >99 | 17 | 60.5 |
| 12 | Cu/chitosan powder ($Cu(OAc)_2$) | 3.4 | >99 | 74 | 59.1 |

[a] Reaction condition: benzylamine (0.5 mmol), TBHP (1.0 mmol), catalyst (10 mg), $CH_3CN$ (2 mL), 80 °C, 30 min. [b] Copper precursor is indicated in the parenthesis, where appropriate. [c] Cu loadings were calculated from copper content in the beads determined by ICP-MS technique. [d] Conversion and yield were determined by GC-MS using hexamethylbenzene (10 mg) as internal standard. [e] Isolated yield.

those of the beads. These results are in good agreement with the low surface area (<5 $m^2$ $g^{-1}$) and total pore volume of Cu/chitosan beads, suggesting that the reaction occurred mainly on the external surface. Nevertheless, the workup process for the powder catalyst was much more tedious and time-consuming as may be anticipated from Fig. 9.

The reaction parameters including solvent, temperature, and oxidizing agent can also affect the catalytic performance of Cu/chitosan beads. Cu/chitosan beads prepared from $Cu(OAc)_2$ with 11% copper content were employed in the evaluation of the reaction parameters summarized in Table S2.† Under solvent-free condition, the oxidative coupling of benzylamine at 80 °C using TBHP as the oxidizing agent afforded 98% yield in just 10 min, but the fracture of the catalyst beads could be observed. Likewise, when using toluene, DMSO, EtOAc, and water as the solvent, the beads were misshapen. Among the studied solvents, the reaction in acetonitrile proceeded smoothly and provided the best catalytic results (Table S2,† entry 3). The effect of the oxidizing agents is also demonstrated in Table S2,† entries 9–11. Under static ambient and oxygen bubbling, the coupling reaction in acetonitrile at 80 °C was slow with 12 and 14% yield of imine at 30 min. Hydrogen peroxide gave a moderate yield (46%) of imine; however, the beads were shattered into small pieces during the reaction. Then, the reaction was carried out with the mild and versatile oxidizing agent, *tert*-butyl hydroperoxide (TBHP), which improved the reaction yield to 98%, and the spherical shape of the catalyst beads was preserved. The reaction temperature was also varied from 30 to 90 °C as illustrated in Table S2,† entries 12–14. As expected, the yield could be raised with increasing temperature. Lastly, the effect of the catalyst loading was studied (Table S2,† entries 15–17). Increasing the catalyst loading from 5 to 10 mg, the yield at 30 min rose significantly from 73 to 98%. The further addition of Cu/chitosan bead catalyst did not improve the yield at 30 min. Therefore, the most suitable reaction condition is to perform the oxidative coupling of benzylamine in acetonitrile at 80 °C for 30 min with TBHP as the oxidizing agent and 10 mg of Cu/chitosan beads derived from $Cu(OAc)_2$ as the catalyst to obtain 98% yield of the imine product.

To evaluate the versatility of Cu/chitosan bead catalyst, the scope of substrates was extended. A variety of structurally diverse primary amines efficiently underwent oxidation to provide corresponding imine products (Table 2). Excellent catalytic activities were observed for benzylamine derivatives (entries 1–6). When a methyl substituent was present at different positions on the aromatic ring, similar results were obtained (entries 2–4) so the steric on benzylic ring does not much affect the activity. Furthermore, the oxidative couplings of heteroatom-containing and more steric amines could proceed selectively to afford the products in 74–92% yield (entries 7–13).

The oxidative cross-coupling of various amines is an important process to further expand the oxidative coupling synthetic methodology for the preparation of diverse imines, particularly the unsymmetrical ones. Cu/chitosan beads were subsequently utilized as a catalyst in the oxidative cross-coupling of amines to imines (Table 3). The reaction between benzylamine and aniline gave 95% yield of the target product as shown in entry 1. However, the catalytic activities between aniline derivatives or aliphatic amine and benzylamine provided only moderate yields as depicted in entries 2–6. The steric hindrance of aniline derivatives influences the reactivity more than the substituent on benzylamine. Therefore, at the same reaction time, higher yields were observed for the coupling between aniline and benzylamine derivatives (entries 7–11). The steric effect around reacting site should be the main factor for the declining reactivity. The substrate with a substituent at the para position provided higher yield than those at the *meta* and *ortho* positions, respectively (entries 7–9).

Table 2 The oxidative self-coupling reaction of benzylamine derivatives[a]

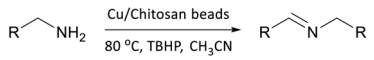


| Entry | Product | Reaction time | Yield[b] (%) |
|---|---|---|---|
| 1 | 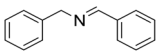 | 30 min | 99 |
| 2 | 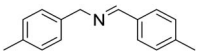 | 30 min | 96 |
| 3 | 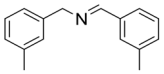 | 30 min | 95 |
| 4 | 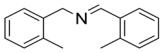 | 30 min | 95 |
| 5 | 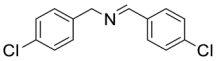 | 30 min | 87 |
| 6 | 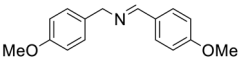 | 30 min | 94 |
| 7 | 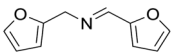 | 3 h | 92 |
| 8 | 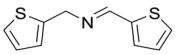 | 30 min | 81 |
| 9 | 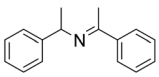 | 30 min | 74 |
| 10 | 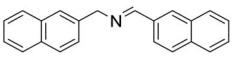 | 1 h | 87 |
| 11 | 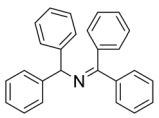 | 30 min | 95 |
| 12 | 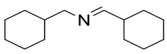 | 1.5 h | 78 |
| 13 | 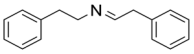 | 1 h | 94 |
| 14 | 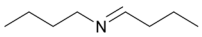 | 1.5 h | 26 |

[a] Reaction condition: benzylamine derivatives (0.5 mmol), TBHP (1.0 mmol), Cu/chitosan beads (10 mg), $CH_3CN$ (2 mL), 80 °C. [b] Determined by $^1H$ NMR using hexamethylbenzene (5 mg) as internal standard.

Table 3 The oxidative cross-coupling reaction between benzylamine derivatives and aniline derivatives[a]

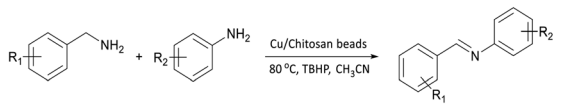


| Entry | Product | Yield[b] (%) |
|---|---|---|
| 1 | 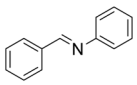 | 95 |
| 2 | 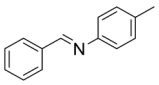 | 66 |
| 3 | 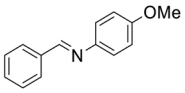 | 61 |
| 4 | 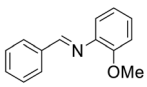 | 54 |
| 5 | 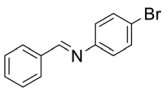 | 88 |
| 6 | 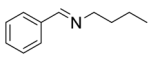 | 65 |
| 7 | 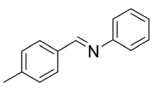 | 91 |
| 8 | 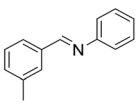 | 89 |
| 9 | 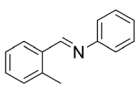 | 81 |
| 10 | 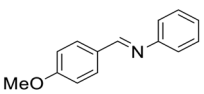 | 84 |
| 11 | 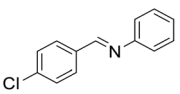 | 94 |

[a] Reaction condition: benzylamine derivatives (0.5 mmol), aniline derivatives (1.5 mmol), TBHP (1.0 mmol), Cu/chitosan beads (10 mg), $CH_3CN$ (2 mL), 80 °C, 24 h. [b] Determined by $^1H$ NMR using hexamethylbenzene (5 mg) as internal standard.

## Reusability of Cu/chitosan beads

The reusability of Cu/chitosan beads in the oxidative self-coupling reaction of benzylamine was tested and the results are shown in Fig. 10. Cu/chitosan beads used in the reaction cycle was separated by simple decantation. After washing with ethyl acetate (3 × 2 mL), the catalyst beads were charged with a new batch of reactants. The separation was very convenient, there was no need to centrifuge or dry the beads before using them in the next reaction cycle. This process demonstrates the

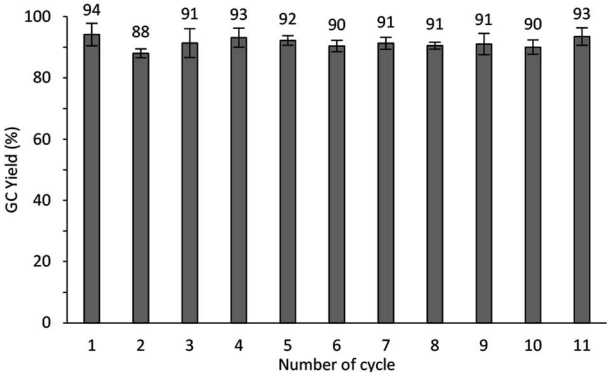


Fig. 10 Reusability of Cu/chitosan beads in the oxidative self-coupling reaction of benzylamine. Reaction condition: benzylamine (0.5 mmol), TBHP (1.0 mmol), Cu/chitosan beads (10 mg), $CH_3CN$ (2 mL), hexamethylbenzene (5 mg), 80 °C, 30 min.

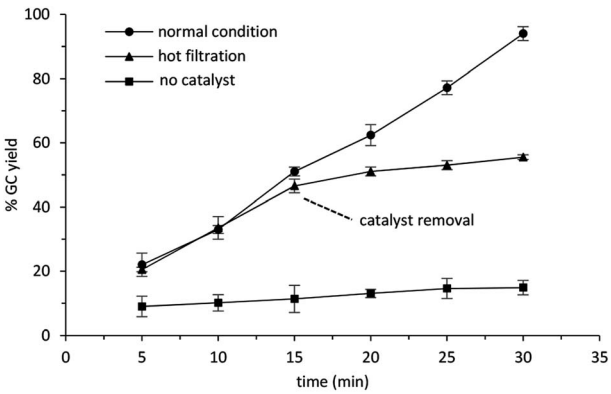


Fig. 11 Hot-filtration test of self-coupling reaction of benzylamine. Reaction condition: benzylamine (0.5 mmol), TBHP (1.0 mmol), Cu/chitosan beads (10 mg), $CH_3CN$ (2 mL), hexamethylbenzene (5 mg), 80 °C.

advantage of the catalyst beads over powders. Moreover, the results showed that Cu/chitosan beads can be reused more than ten cycles without losing their performance. SEM images (Fig. S4†) reveal that Cu/chitosan beads still retained the bead structure after uses, even though the surface texture of the beads appeared rougher after ten cycles. In addition, from ICP-MS results, the copper content in the used catalyst beads was similar to the fresh ones (11%). This evidence verified the stability of the beads, and no copper species leached into the reaction.

A hot-filtration test was performed in the self-coupling reaction of benzylamine with TBHP at 80 °C as demonstrated in Fig. 11. After the catalyst removal at 15 min, no more product was obtained, suggesting that there was no leaching of any active species during the reaction. Therefore, the catalysis was heterogeneous in nature.

## Comparison of catalytic activity

Among the results for the catalytic oxidative self-coupling of benzylamine, the best condition is to carry out the reaction at

Table 4 Comparison of various heterogeneous catalysts for oxidative self-coupling of benzylamine

| Entry | Catalyst | Condition | TOF[a] ($h^{-1}$) | Conversion (%) | Selectivity (%) | Yield (%) | Reusability[b] (cycle) | Ref. |
|---|---|---|---|---|---|---|---|---|
| 1 | Cu/chitosan beads | 80 °C, acetonitrile, 30 min, TBHP in decane | 57.7 | >99 | >99 | 98 | 11 | This work |
| 2 | $Cu/Al_2O_3$ | 150 °C, *p*-xylene, 24 h | 0.6 | 80 | >99 | — | 2 | 43 |
| 3 | $CuO/Al_2O_3$ | 110 °C, toluene, 24 h | 2.0 | — | — | 97 | — | 40 |
| 4 | Cu (red copper) | 100 °C, toluene, 24 h, $NH_4Br$, 10-phenanthroline | 0.3 | 97 | >99 | 97 | — | 42 |
| 5 | Cu powder | 90 °C, solvent-free, 20 h | 9.3 | >99 | >99 | >99 | — | 44 |
| 6 | $CuO–CeO_2$ | 110 °C, DMSO, 22 h | 0.9 | — | — | 90 | 2 | 41 |
| 7 | Cu/HMPC | 80 °C, solvent-free, 4.5 h | 36 | — | — | 98 | 4 | 33 |
| 8 | $Cu_{meth}Al_{butox}$ | 100 °C, solvent-free, 15 h | 0.36 | >99 | >99 | — | — | 34 |
| 9 | Cu–GO@*m*-$SiO_2$ | 110 °C, solvent-free, 12 h | — | 98 | 97 | — | 4 | 35 |
| 10 | K-10 Montmorillonite | 150 °C, solvent-free, 3 min, microwaves | — | — | — | 80 | — | 38 |
| 11 | α-$MnO_2$ | 25 °C, acetonitrile, 4 h, TBHP in decane | 2.5 | >99 | 95 | — | — | 50 |
| 12 | MOF-253 | 100 °C, solvent-free, 6 h | — | >99 | >99 | 99 | 6 | 51 |
| 13 | Nanogold/SBA-15 | 85 °C, solvent-free, 4 h, TBHP in water | 172.3 | 98 | 99 | — | 5 | 28 |
| 14 | AuNPs/SBA-$NH_2$ | 100 °C, toluene, 24 h | 14.3 | 92 | 98 | 90 | 5 | 27 |
| 15 | Ce–Sm/$SiO_2$ | 120 °C, solvent-free, 6 h, $O_2$ bubble | — | >99 | >99 | — | 4 | 29 |
| 16 | Mesoporous carbon | 120 °C, solvent-free, 24 h | — | — | >99 | 94 | 5 | 52 |

[a] TOF is the number of moles of reactant consumed per mole of Cu per unit of time. [b] "—" = Data not available.

80 °C for 30 min by using 10 mg of Cu/chitosan beads derived from $Cu(OAc)_2$ in the presence of TBHP as the oxidizing agent and acetonitrile as the solvent. The reaction achieved 99% conversion and 98% yield. In Table 4, the catalytic efficiency is illustrated and compared with other copper catalysts (entries 2–9) as well as other metal-based catalysts (entries 10–16). Even though it is difficult to directly compare the results due to the different reaction conditions, our Cu/chitosan bead system exhibited satisfactory catalytic activity with short reaction time and could be reused for many cycles with no loss of activity.

## Conclusions

In conclusion, we have developed, nonprecious metal and biopolymer-based catalyst, Cu/chitosan beads, by using a software-controlled flow system. The size and morphology of the Cu/chitosan beads are reproducible due to high precision of the flow rate. Furthermore, the Cu/chitosan beads can catalyze the oxidation of diverse types of amines to corresponding imines in moderate to high yields under short reaction time. Because of the bead morphology, these catalysts greatly simplify the operation and workup procedures. In the recycle process, after decantation and washing, the Cu/chitosan beads could be reused without drying. Importantly, the beads could be recycled more than ten times without an appreciable loss of the catalytic performance. Finally, the procedure to prepare Cu/chitosan beads is expected to contribute to the development of new catalyst systems and the application to other reactions.

## Conflicts of interest

There are no conflicts of interest to declare.

## Acknowledgements

We would like to thank the Royal Golden Jubilee PhD Scholarship (PHD/0171/2556) from the Thailand Science Research and Innovation (TSRI). Financial support from the Center of Excellence for Innovation in Chemistry (PERCH-CIC), Ministry of Higher Education, Science, Research and Innovation is gratefully acknowledged. We also thank the Center for Nanoimaging (CNI) and the Central Instrument Facility (CIF Grant), Faculty of Science, Mahidol University, for assistance on microscopy experiment and for instrumentation supports, respectively.

## References

1 A. V. Kucherov, N. V. Kramareva, E. D. Finashina, A. E. Koklin and L. M. Kustov, Heterogenized redox catalysts on the basis of the chitosan matrix: 1. copper complexes, *J. Mol. Catal. A: Chem.*, 2003, **198**, 377–389.
2 D. J. Macquarrie and J. J. E. Hardy, Applications of functionalized chitosan in catalysis, *Ind. Eng. Chem. Res.*, 2005, **44**, 8499–8520.
3 E. Guibal, Heterogeneous catalysis on chitosan-based materials: a review, *Prog. Polym. Sci.*, 2005, **30**, 71–109.
4 A. El Kadib, Chitosan as a sustainable organocatalyst: a concise overview, *ChemSusChem*, 2015, **8**, 217–244.

 

5 Á. Molnár, The use of chitosan-based metal catalysts in organic transformations, *Coord. Chem. Rev.*, 2019, **388**, 126–171.
6 Anuradha, S. Kumari and D. D. Pathak, Synthesis and development of chitosan anchored copper(II) schiff base complexes as heterogeneous catalysts for *N*-arylation of amines, *Tetrahedron Lett.*, 2015, **56**, 4135–4142.
7 P. Xu, B. Li, L. Wang, C. Qin and L. Zhu, A green and recyclable chitosan supported catalyst for the borylation of α,β-unsaturated acceptors in water, *Catal. Commun.*, 2016, **86**, 23–26.
8 X. Liu, S. Chang, X. Chen, X. Ge and C. Qian, Efficient Ullmann C–X coupling reaction catalyzed by a recoverable functionalized-chitosan supported copper complex, *New J. Chem.*, 2018, **42**, 16013–16020.
9 C. Shen, J. Xu, W. Yu and P. Zhang, A highly active and easily recoverable chitosan@copper catalyst for the C-S coupling and its application in the synthesis of zolimidine, *Green Chem.*, 2014, **16**, 3007–3012.
10 C. Bodhak, A. Kundu and A. Pramanik, An efficient and recyclable chitosan supported copper(II) heterogeneous catalyst for C–N cross coupling between aryl halides and aliphatic diamines, *Tetrahedron Lett.*, 2015, **56**, 419–424.
11 O. Jennah, R. Beniazza, C. Lozach, D. Jardel, F. Molton, C. Duboc, T. Buffeteau, A. El Kadib, D. Lastécouères, M. Lahcini and J.-M. Vincent, Photoredox catalysis at copper(II) on chitosan: application to photolatent CuAAC, *Adv. Synth. Catal.*, 2018, **360**, 4615–4624.
12 R. B. N. Baig and R. S. Varma, Copper on chitosan: a recyclable heterogeneous catalyst for azide-alkyne cycloaddition reactions in water, *Green Chem.*, 2013, **15**, 1839–1843.
13 M. Chetia, A. A. Ali, D. Bhuyan, L. Saikia and D. Sarma, Magnetically recoverable chitosan-stabilised copper-iron oxide nanocomposite material as an efficient heterogeneous catalyst for azide-alkyne cycloaddition reactions, *New J. Chem.*, 2015, **39**, 5902–5907.
14 A. Intanin, P. Inpota, T. Chutimasakul, J. Tantirungrotechai, P. Wilairat and R. Chantiwas, Development of a simple reversible-flow method for preparation of micron-size chitosan-Cu(II) catalyst particles and their testing of activity, *Molecules*, 2020, **25**, 1798.
15 C. M. da Silva, D. L. da Silva, L. V. Modolo, R. B. Alves, M. A. de Resende, C. V. B. Martins and Â. de Fátima, Schiff bases: a short review of their antimicrobial activities, *J. Adv. Res.*, 2011, **2**, 1–8.
16 P. G. Cozzi, Metal-salen schiff base complexes in catalysis: practical aspects, *Chem. Soc. Rev.*, 2004, **33**, 410–421.
17 B. Chen, L. Wang and S. Gao, Recent advances in aerobic oxidation of alcohols and amines to imines, *ACS Catal.*, 2015, **5**, 5851–5876.
18 G. Chu and C. Li, Convenient and clean synthesis of imines from primary benzylamines, *Org. Biomol. Chem.*, 2010, **8**, 4716–4719.
19 X. Jia, J. Ma, F. Xia, M. Gao, J. Gao and J. Xu, Switching acidity on manganese oxide catalyst with acetylacetones for selectivity-tunable amines oxidation, *Nat. Commun.*, 2019, **10**, 2338.
20 S.-S. Kim, S. Thakur, J.-Y. Song and K.-h. Lee, Oxidative coupling of benzylamines into *N*-benzylbenzaldimines with Mn(II)/*tert*-BuOOH, *Bull. Korean Chem. Soc.*, 2005, **26**, 499–501.
21 S. Hazra, P. Pilania, M. Deb, A. K. Kushawaha and A. J. Elias, Aerobic oxidation of primary amines to imines in water using a cobalt complex as recyclable catalyst under mild conditions, *Chem.–Eur. J.*, 2018, **24**, 15766–15771.
22 C. Zhang, P. Zhao, Z. Zhang, J. Zhang, P. Yang, P. Gao, J. Gao and D. Liu, Co–N–C supported on $SiO_2$: a facile, efficient catalyst for aerobic oxidation of amines to imines, *RSC Adv.*, 2017, **7**, 47366–47372.
23 M. Aman, J. Tremmel, L. Dostál, M. Erben, J. Tydlitát, J. Jansa and R. Jambor, Highly active and selective Ru-PNH catalyst in aerobic oxidation of benzyl amines, *ChemCatChem*, 2019, **11**, 4624–4630.
24 R. E. Rodríguez-Lugo, M. A. Chacón-Terán, S. De León, M. Vogt, A. J. Rosenthal and V. R. Landaeta, Synthesis, characterization and Pd(II)-coordination chemistry of the ligand *tris*(quinolin-8-yl)phosphite. Application in the catalytic aerobic oxidation of amines, *Dalton Trans.*, 2018, **47**, 2061–2072.
25 C. Ge, X. Sang, W. Yao, L. Zhang and D. Wang, Unsymmetrical indazolyl-pyridinyl-triazole ligand-promoted highly active iridium complexes supported on hydrotalcite and its catalytic application in water, *Green Chem.*, 2018, **20**, 1805–1812.
26 C. M. Opris, O. D. Pavel, A. Moragues, J. El Haskourib, D. Beltran, P. Amoros, M. D. Marcos, L. E. Stoflea and V. I. Parvulescu, New multicomponent catalysts for the selective aerobic oxidative condensation of benzylamine to *N*-benzylidenebenzylamine, *Catal. Sci. Technol.*, 2014, **4**, 4340–4355.
27 C. K. P. Neeli, S. Ganji, V. S. P. Ganjala, S. R. R. Kamaraju and D. R. Burri, Oxidative coupling of primary amines to imines under base-free and additive-free conditions over AuNPs/SBA-$NH_2$ nanocatalyst, *RSC Adv.*, 2014, **4**, 14128–14135.
28 C. K. P. Neeli, M. Ravi Kumar, G. Saidulu, K. S. Rama Rao and D. R. Burri, Selective oxidation of benzylamine to *N*-benzyl benzaldimine over nanogold immobilized SBA-15 under solvent-free conditions, *J. Chem. Technol. Biotechnol.*, 2015, **90**, 1657–1664.
29 P. Sudarsanam, A. Rangaswamy and B. M. Reddy, An efficient noble metal-free Ce-Sm/$SiO_2$ nano-oxide catalyst for oxidation of benzylamines under ecofriendly conditions, *RSC Adv.*, 2014, **4**, 46378–46382.
30 J. Kim, G. Golime, H. Y. Kim and K. Oh, Copper(II)-catalyzed aerobic oxidation of amines: divergent reaction pathways by solvent control to imines and nitriles, *Asian J. Org. Chem.*, 2019, **8**, 1674–1679.
31 S. Elavarasan, A. Bhaumik and M. Sasidharan, An efficient mesoporous Cu-organic nanorod for Friedländer synthesis of quinoline and click reactions, *ChemCatChem*, 2019, **11**, 4340–4350.

32 R. Jangir, M. Ansari, D. Kaleeswaran, G. Rajaraman, M. Palaniandavar and R. Murugavel, Unprecedented copper(II) complex with a topoquinone-like moiety as a structural and functional mimic for copper amine oxidase: role of copper(II) in the genesis and amine oxidase activity, *ACS Catal.*, 2019, **9**, 10940–10950.

33 M. Gopiraman, K. Wei, K.-Q. Zhang, I.-M. Chung and I. S. Kim, Cultivation of a Cu/HMPC catalyst from a hyperaccumulating mustard plant for highly efficient and selective coupling reactions under mild conditions, *RSC Adv.*, 2018, **8**, 4531–4547.

34 D. Dissanayake, L. A. Achola, P. Kerns, D. Rathnayake, J. He, J. Macharia and S. L. Suib, Aerobic oxidative coupling of amines to imines by mesoporous copper aluminum mixed metal oxides via generation of Reactive Oxygen Species (ROS), *Appl. Catal., B*, 2019, **249**, 32–41.

35 C. Sarkar, S. Pendem, A. Shrotri, D. Q. Dao, P. Pham Thi Mai, T. Nguyen Ngoc, D. R. Chandaka, T. V. Rao, Q. T. Trinh, M. P. Sherburne and J. Mondal, Interface engineering of graphene-supported Cu nanoparticles encapsulated by mesoporous silica for size-dependent catalytic oxidative coupling of aromatic amines, *ACS Appl. Mater. Interfaces*, 2019, **11**, 11722–11735.

36 M. Largeron and M.-B. Fleury, A metalloenzyme-like catalytic system for the chemoselective oxidative cross-coupling of primary amines to imines under ambient conditions, *Chem.–Eur. J.*, 2015, **21**, 3815–3820.

37 Z. Hu and F. M. Kerton, Simple copper/TEMPO catalyzed aerobic dehydrogenation of benzylic amines and anilines, *Org. Biomol. Chem.*, 2012, **10**, 1618–1624.

38 K. Marui, A. Nomoto, M. Ueshima and A. Ogawa, Eco-friendly copper sulfate-catalyzed oxidation of amines to imines by hydrogen peroxide in water, *Tetrahedron Lett.*, 2015, **56**, 1200–1202.

39 B. Huang, H. Tian, S. Lin, M. Xie, X. Yu and Q. Xu, Cu(I)/TEMPO-catalyzed aerobic oxidative synthesis of imines directly from primary and secondary amines under ambient and neat conditions, *Tetrahedron Lett.*, 2013, **54**, 2861–2864.

40 Y. F. Wang, J. H. Zeng and X. R. Cui, CuO-$Al_2O_3$ catalyzed oxidation of primary benzylamines and secondary dibenzylamines to *N*-benzylbenzaldimines, *Org. Commun.*, 2013, **6**, 68–77.

41 L. Al-Hmoud and C. W. Jones, Reaction pathways over copper and cerium oxide catalysts for direct synthesis of imines from amines under aerobic conditions, *J. Catal.*, 2013, **301**, 116–124.

42 J. Wang, S. Lu, X. Cao and H. Gu, Common metal of copper(0) as an efficient catalyst for preparation of nitriles and imines by controlling additives, *Chem. Commun.*, 2014, **50**, 5637–5640.

43 H. Liu, G.-K. Chuah and S. Jaenicke, Self-coupling of benzylamines over a highly active and selective supported copper catalyst to produce *N*-substituted amines by the borrowing hydrogen method, *J. Catal.*, 2015, **329**, 262–268.

44 R. D. Patil and S. Adimurthy, Copper(0)-catalyzed aerobic oxidative synthesis of imines from amines under solvent-free conditions, *RSC Adv.*, 2012, **2**, 5119–5122.

45 K. Tokarek, J. L. Hueso, P. Kuśtrowski, G. Stochel and A. Kyzioł, Green synthesis of chitosan-stabilized copper nanoparticles, *Eur. J. Inorg. Chem.*, 2013, 4940–4947.

46 Y. w. fen, W. M. Mat Yunus, Z. Talib and N. Yusof, X-ray photoelectron spectroscopy and atomic force microscopy studies on crosslinked chitosan thin film, *Int. J. Phys. Sci.*, 2011, **6**, 2744–2749.

47 R. S. Vieira, M. L. M. Oliveira, E. Guibal, E. Rodríguez-Castellón and M. M. Beppu, Copper, mercury and chromium adsorption on natural and crosslinked chitosan films: an XPS investigation of mechanism, *Colloids Surf., A*, 2011, **374**, 108–114.

48 S. Basumallick, P. Rajasekaran, L. Tetard and S. Santra, Hydrothermally derived water-dispersible mixed valence copper-chitosan nanocomposite as exceptionally potent antimicrobial agent, *J. Nanopart. Res.*, 2014, **16**, 2675.

49 E. T. Valdés and G. C. Triviño, Chitosan metal complexes and chitosan-Cu ESR studies, *J. Chil. Chem. Soc.*, 2009, **54**, 1–5.

50 Z. Zhang, F. Wang, M. Wang, S. Xu, H. Chen, C. Zhang and J. Xu, *tert*-Butyl hydroperoxide (TBHP)-mediated oxidative self-coupling of amines to imines over a $\alpha$-$MnO_2$ catalyst, *Green Chem.*, 2014, **16**, 2523–2527.

51 X. Qiu, C. Len, R. Luque and Y. Li, Solventless oxidative coupling of amines to imines by using transition-metal-free metal-organic frameworks, *ChemSusChem*, 2014, **7**, 1684–1688.

52 B. Chen, L. Wang, W. Dai, S. Shang, Y. Lv and S. Gao, Metal-free and solvent-free oxidative coupling of amines to imines with mesoporous carbon from macrocyclic compounds, *ACS Catal.*, 2015, **5**, 2788–2794.

 